ELSEVIER

Journal of Hazardous Materials 141 (2007) 123–127

Journal of Hazardous Materials

www.elsevier.com/locate/jhazmat

Photocatalytic degradation of textile dye X-3B using polyoxometalate–TiO_2 hybrid materials

Hongxiao Jin [a], Qingyin Wu [a,*], Wenqin Pang [a,b,**]

[a] *Department of Chemistry, Zhejiang University, Hangzhou 310027, PR China*
[b] *State Key Laboratory of Inorganic Synthesis and Preparative Chemistry, Department of Chemistry, Jilin University, Changchun 130023, PR China*

Received 12 July 2005; received in revised form 26 June 2006; accepted 26 June 2006
Available online 1 July 2006

Abstract

Titanium dioxide functionalized with Keggin type polyoxometalate (POMs) $[X^{n+}W_{12}O_{40}]^{(8-n)-}$ (XW_{12}; $X^{n+} = P^{5+}$, Si^{4+}, Ge^{4+}) were prepared by sol–gel method. The Keggin structure and dispersion state of POMs were monitored by FT-IR and XRD. The composites showed higher photocatalytic activity than pure TiO_2, pure POMs or mechanical mixture of TiO_2 and POMs for X-3B degradation. Among the three POMs–TiO_2 hybrid materials, the reactivity was: $PW_{12} > SiW_{12} > GeW_{12}$. With different loading weights for the same POMs, the reactivity followed the order: 30 wt.% > 15 wt.% > 45 wt.%.

Keywords: Polyoxometalate; Titanium dioxide; Sol–gel; Photocatalytic degradation

1. Introduction

The increasing organic compounds in wastewater has raised serious environmental problem [1]. Various methods have been used to degrade or remove these contaminates by physical, chemical, photochemical and microbiological process [2,3]. Semiconductors (TiO_2, ZnO, Fe_2O_3, SnO_2, WO_3, etc.) act as photocatalysts in photochemical process have received a great deal of attention for their potential to utilize the solar photons [4,5]. There are a number of similarities between polyoxometalates (POMs) and semiconductor mental oxides [6]. The photochemistry of POMs can be regarded as a model for the photochemical processes on semiconductor mental oxides surfaces. The major drawback of POM photocatalytic system is the high solubility of the POMs, which impedes the recovery and reuse of the catalysts. Incorporation of POMs into the solid matrix is interesting because the support makes POMs easily handled and recycled. Moreover, most supported POMs have micro- or mesoporous structures, the photocatalytic activity of these porous solid was expected to be increase significantly due to their much higher surface areas compared with their parent POMs [7].

In this contribution, we discuss the sol–gel synthesis of highly dispersed POMs species in the TiO_2 substrate. Main motivations of design these materials are: (1) improvement of the photocatalytic activity of pure POMs through dispersion of POMs into the TiO_2 solid; (2) separation and recovery of the photocatalysts from the reaction environments became easy; (3) combination of these two materials having much higher photocatalytic activity than their pure form due to the synergistic effect [8–11]. Three types of POMs ($H_3PW_{12}O_{40}$, $H_4SiW_{12}O_{40}$ and $H_4GeW_{12}O_{40}$) with Keggin structure are used and the weight ratio of POMs in the TiO_2 matrix is adjusted (15, 30 and 45 wt.%). FT-IR and XRD spectroscopy are used to elucidate the structure and the dispersion state of the supported POMs. All these samples have been tested by photocatalytic degradation of reactive brilliant red X-3B. Table 1 shows the characteristic of the Reactive brilliant red X-3B. This textile dyes is commonly used in industry. We study the photodegradation of X-3B by XW_{12}–TiO_2 (X = P, Si and Ge) as to find more simple and economic method for treating this dye-containing wastewater.

* Corresponding author. Tel.: +86 571 87953258; fax: +86 571 87951895.
** Corresponding author. Tel.: +86 431 5168590; fax: +86 431 5168590.
E-mail addresses: qywu@zju.edu.cn (Q. Wu), wqpang@mail.jlu.edu.cn (W. Pang).

0304-3894/$ – see front matter © 2006 Elsevier B.V. All rights reserved.
doi:10.1016/j.jhazmat.2006.06.098

Table 1
The characteristic of the reactive brilliant red X-3B

Commercial name	Reactive brilliant red X-3B
Structural formula	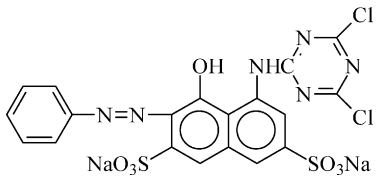
IUPAC name	2,7-Naphthalenedisulfonic acid, 5-((4,6-dichloro-s-triazin-2-yl) amino)-4-hydroxy-3-(phenylazo)-, disodium salt
C.A.S. number	17804-49-8
Color index name	Reactive red 2
Color index number	18200
Color index category	Reactive dye
Class	Monoazo (reactive system: dichlorotriazinyl)
Synonyms	Brilliant Red 5SKH, Cerven reaktivni 2 (Czech), Chemictive Brilliant Red 5B, Mikacion Brilliant Red 5BS, Brilliant Red S 5B, Procion Brilliant Red 5BS, Procion Brilliant Red M 5B
Formula weight	615.34
Formula hill	C19H13Cl2N6NaO7S2
Absorb. (max) UV/vis (in water)	538 nm
Melting point	300 °C
Boiling point	N.A.
Solubility in water	70 g/L
L.D.50 oral (in rat)	7460 mg/kg
Use	Textile use: dye for cellulose, nylon, silk and wool

2. Experimental

2.1. Materials

Titanium isopropoxide ($Ti(O\text{-}^{i}Pr)_4$) was purchased from Aldrich Chemical Co. Reactive brilliant X-3B (98%) was from Jining dye manufacture of China, and used directly without further purification. 12-Tungstophosphoric acid ($H_3PW_{12}O_{40}\cdot 6.7H_2O$), 12-tungstosilicatic acid ($H_4SiW_{12}O_{40}\cdot 26H_2O$) and 12-tungstogermanic acid ($H_4GeW_{12}O_{40}\cdot 14H_2O$) were prepared according to the literature methods [12]. TiO_2 (mainly of anatase form conformed by XRD, BET area: ca. 11 $m^2\,g^{-1}$), $HClO_4$ and H_2O_2 were from Shanghai Chemicals of China and used as received. Double distilled water was used throughout the process.

2.2. Preparation of the materials

POMs anchored TiO_2 gel was prepared by sol–gel method. Appropriate amount of POMs was dissolved in 20 ml of 2-methoxy-ethanol, 5 ml of TIP was added drop wise to this solution with stir. In the first stage, precipitation of titanium was observed, by adding more, complete re-dissolution occurred and an orange solution was achieved. Viscous yellow gels were prepared by removing volatile components on a rotary evaporator at ambient temperature. The samples were denoted as (S)-$XW_{12}(Y)$–TiO_2. The X (X = P, Si and Ge) represents the different type of POMs and Y (Y = 15, 30 and 45) refers to the loading amounts of POMs as wt.%. These amounts were controlled by changing the weight of the POMs solid and assumed from the preparative recipe. Also a series of mechanically mixed sample denoting as (M)-$XW_{12}(Y)$–TiO_2 were prepared by incipient wetness method for comparing.

2.3. Characterization and photocatalytic testing

X-ray diffraction patterns were obtained with a Siemens D5005 diffractometer using Cu Kα radiation ($\lambda = 0.15418$ nm). FT-IR spectra were recorded on a Nicollet Impact 410 FT-IR spectrometer using KBr pellets.

The apparatus for photocatalytic testing could be found elsewhere [13]. A general photocatalytic procedure was carried out as follows: 0.05 g of catalyst POMs/TiO_2 was suspended in a fresh aqueous X-3B (6.37×10^{-5} M, pH 1.0) solution. The suspension (50 ml) was ultrasonicated for 5 min and stirred in the dark for 2 h to obtain a good dispersion and establish adsorption–desorption equilibrium between the dye and the surface of the catalyst. The degradation experiment was carried out after the lamp was stable. The suspension was opened to the air and vigorously stirred during the process. Decreasing in the concentration of dye was monitored by a 722 spectrophotometer (Shanghai Analytical Instrument Factory).

3. Results and discussion

3.1. Characterization of POMs–TiO_2

3.1.1. Preservation of Keggin structure in the hybrid materials

Pure Keggin units displayed characteristic infrared fingerprints in the region from 1100 to 500 cm^{-1} (dot lines in Fig. 1), the FT-IR spectra of pure POMs showed fundamentals at 1080, 982, 889, 800, 596, 525 cm^{-1} for PW_{12}, 1018, 980, 926, 881, 785, 540 cm^{-1} for SiW_{12} and 978, 889, 827, 773, 532, 463 cm^{-1} for GeW_{12}. These attributed to the vibration of X-O in the central XO_4 units and W–O–W of XW_{12}. Assignments of peaks were based on literature values [14] and cataloged in Table 2. The spectra of XW_{12}–TiO_2 (solid lines in Fig. 1) showed an intense, broad, indistinct region extending from 1100 to 400 cm^{-1} attributable to TiO_2 [15]. FT-IR spectroscopy was commonly used to determine the presence of the POMs cluster on the surface of substrates [16]. Similar vibration bands to the corresponding XW_{12} structures could be found in all XW_{12}–TiO_2 samples, suggesting the remaining of the Keggin structure. Red or blue peak shifts were observed in all the sol–gel derived samples. The max shift number was found in ν_{as}(W–O_c–W) peak, which was about 20, 21, 14 cm^{-1} for X = P, Si and W, respectively. The intensity of the ν_{as} (W–O) bands was almost proportional to the amount of XW_{12} on TiO_2 due to the greater numbers of oscillators. But no such peak shifts were found in mechanical mixtures, indicating the attachment of POMs on the surface of TiO_2 was weaker in these samples than in (S)-XW_{12}–TiO_2. The peak positions in (S)-XW_{12}–TiO_2 were comparable with pure XW_{12} in aqueous solution [8], and

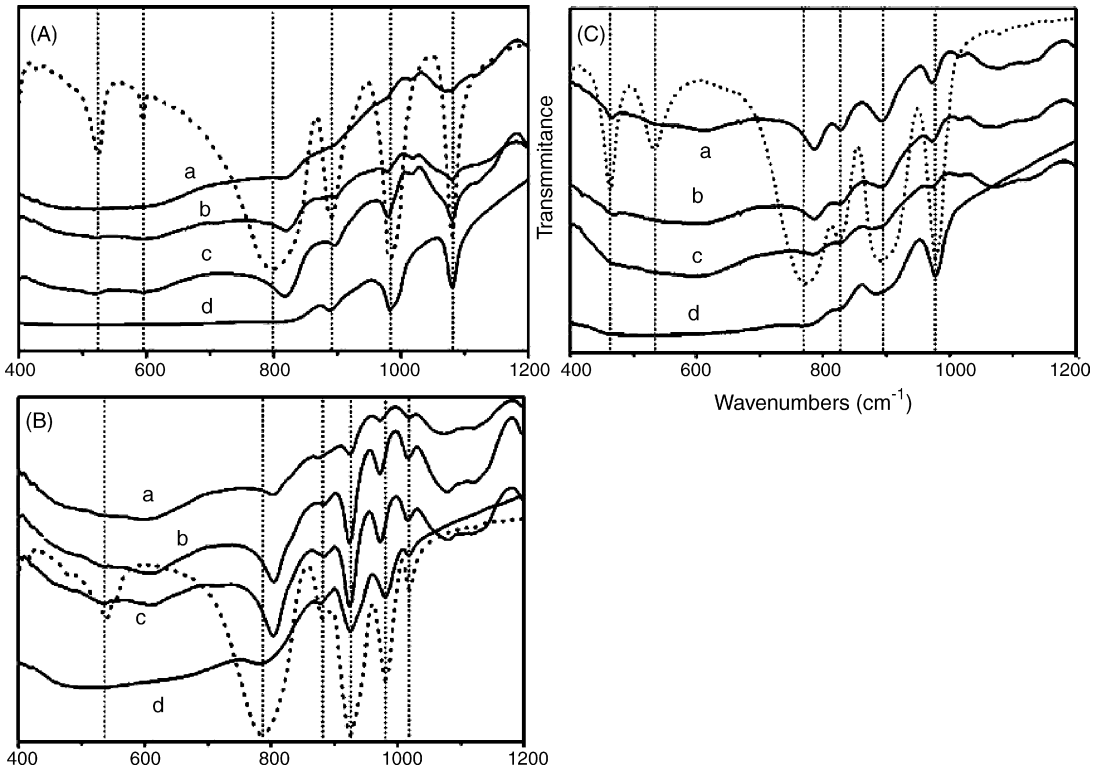

Fig. 1. FT-IR spectra of (A) pure PW_{12} (dot-line), (a) (S)-PW_{12}(15)–TiO_2, (b) (S)-PW_{12}(30)–TiO_2, (c) (S)-PW_{12}(45)–TiO_2, and (d) (M)-PW_{12}(30)–TiO_2; (B) pure SiW_{12} (dot-line), (a) (S)-SiW_{12}(15)–TiO_2, (b) (S)-SiW_{12}(30)–TiO_2, (c) (S)-SiW_{12}(45)–TiO_2, and (d) (M)-SiW_{12}(30)–TiO_2; (C) pure GeW_{12} (dot-line), (a) (S)-GeW_{12}(15)–TiO_2, (b) (S)-GeW_{12}(30)–TiO_2, (c) (S)-GeW_{12}(45)–TiO_2, and (d) (M)-GeW_{12}(30)–TiO_2.

the peak positions in (M)-XW_{12} fitted well with solid pure XW_{12} [14].

3.1.2. Dispersion of POMs

POMs could be supported as molecules or aggregates [16] on the TiO_2 substrate. Fig. 2 shows the X-ray diffraction patterns of the PW_{12}–TiO_2 and PW_{12}. The diffraction peaks from both POMs and TiO_2 could be clearly seen in (M)-PW_{12}(45)–TiO_2 sample (line b), suggesting the aggregation of POMs in the mechanically mixed PW_{12}–TiO_2 sample and poor dispersion of TiO_2. However, they were very weak in (S)-PW_{12}–TiO_2 samples (lines c–e). This means that most attached POMs did not form aggregates with a sufficient size to exhibit intense diffraction peaks in sol–gel derived samples. The POMs diffraction peaks attributed to its secondary structure were considerably reduced due to high dispersion, but its molecular structure was still maintained (confirmed by FT-IR). Similar results were also found in other POMs loading samples (not

Table 2
Main relevant mid-IR data (cm^{-1}) of the starting XW_{12} (X = P, Si and Ge) and their corresponding hybrid titanium materials

Sample	ν_{as}(X–O) (cm^{-1})	ν_{as}(W–O_b–W) (cm^{-1})	ν_{as}(W–O_c–W) (cm^{-1})	ν_{as}(W–O_d) (cm^{-1})
PW_{12}	1080	889	800	982
(S)-PW_{12}(15)–TiO_2	1080	–	–	–
(S)-PW_{12}(30)–TiO_2	1080	897	820	980
(S)-PW_{12}(45)–TiO_2	1080	895	820	980
(M)-PW_{12}(30)–TiO_2	1080	889	–	982
SiW_{12}	926	881	785	980
(S)-SiW_{12}(15)–TiO_2	924	–	804	972
(S)-SiW_{12}(30)–TiO_2	924	883	804	972
(S)-SiW_{12}(45)–TiO_2	924	883	804	972
(M)-SiW_{12}(30)–TiO_2	926	877	–	980
GeW_{12}	827	889	773	978
(S)-GeW_{12}(15)–TiO_2	827	–	785	972
(S)-GeW_{12}(30)–TiO_2	827	893	787	972
(S)-GeW_{12}(45)–TiO_2	825	891	787	972
(M)-GeW_{12}(30)–TiO_2	827	–	–	978

–: peak overlapped by vibration peaks from TiO_2 [15].

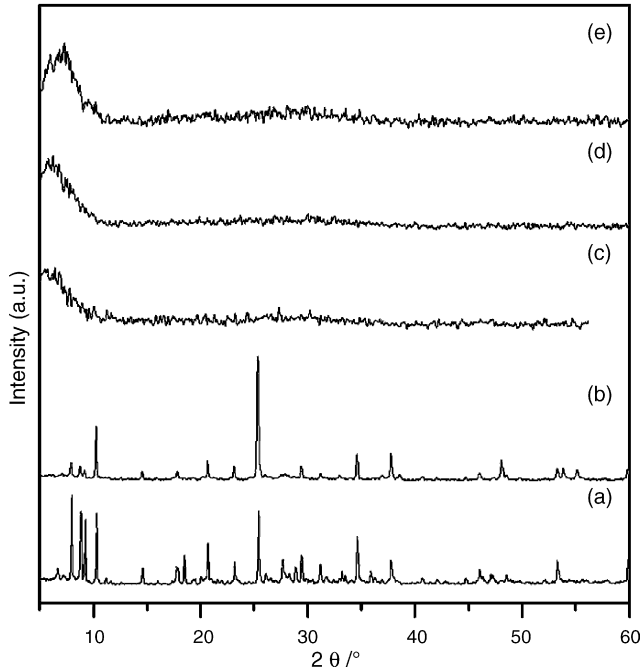

Fig. 2. XRD patterns for pure PW_{12} (a), (M)-PW_{12}(30)–TiO_2 (b), (S)-PW_{12}(15)–TiO_2 (c), (S)-PW_{12}(30)–TiO_2 (d) and (S)-PW_{12}(45)–TiO_2 (e).

shown). The difference in dispersion state consequently affected the photocatalytic performance.

3.2. Photocatalystic reactions

The photocatalytic tests described here were run in aqueous solution containing oxygen. The data fitted well into the first order kinetics [17]. The pH is one of the important factors in application for water treatment. In the present study XW_{12} based materials were employed as the photocatalyst. It was noted that the optimum condition was pH 1 because XW_{12} would partial decomposed into XW_{11} at high pH (>2) [18].

3.2.1. Catalytic activity of XW_{12}–TiO_2 in photodegradation of X-3B

Table 3 shows the photo-degradation of X-3B under various conditions by K_{app} (apparent rate constant). In a separate experiment, it was confirmed that in the absence of photocatalyst the rate of the photoreaction of X-3B was negligible, consistent with previous observation [13]. X-3B underwent more extensive degradation in the presence of XW_{12} under UV irradiation, in agreement with Hu and Xu [19]. However, degradation of this X-3B in TiO_2 dispersion was much faster than in XW_{12} solutions. Mechanically mixing of PW_{12} with TiO_2 resulted in a rate enhancement for X-3B decay (line c in Fig. 3), similar with the results of Ferry et al. [9] and Zhao et al. [10]; but for SiW_{12} and GeW_{12}, the mechanical mixture showed a decrease in reaction rate. The degradation rates significantly improved when (S)-XW_{12}–TiO_2 samples were added. The photocatalytic activity of XW_{12}–TiO_2 was higher than pure POMs and TiO_2, suggesting the degradation of X-3B mainly originates from the synergistic effect by a combination of XW_{12} and TiO_2 [11].

Table 3
Degradation rate constants (min^{-1}) of X-3B photodegradation with 0.1% catalysts loading

Catalyst	K_{obs} (min^{-1})
No catalyst	No detectable reaction
TiO_2	8.64×10^{-3}
Pure PW_{12}	4.01×10^{-4}
Pure SiW_{12}	3.77×10^{-3}
Pure GeW_{12}	1.03×10^{-3}
(M)-PW_{12}(30)–TiO_2	1.07×10^{-2}
(M)-SiW_{12}(30)–TiO_2	4.92×10^{-3}
(M)-GeW_{12}(30)–TiO_2	2.17×10^{-3}
(S)-PW_{12}(30)–TiO_2	6.53×10^{-2}
(S)-SiW_{12}(30)–TiO_2	4.44×10^{-2}
(S)-GeW_{12}(30)–TiO_2	2.78×10^{-2}

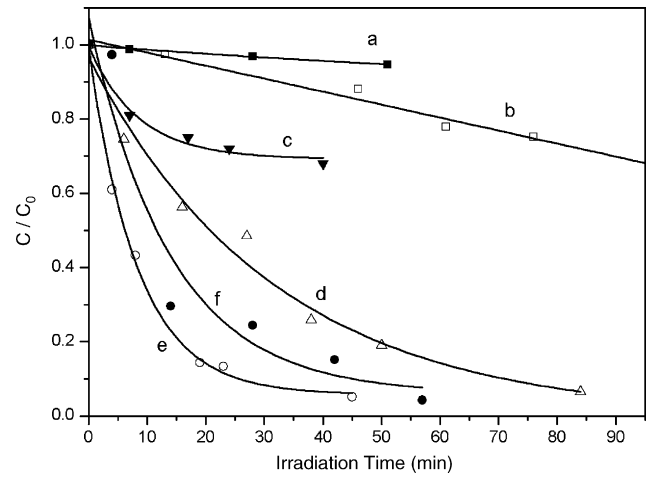

Fig. 3. Degradation of X-3B in presence of $1\,g\,l^{-1}$ (a) PW_{12}, (b) TiO_2, (c) (M)-PW_{12}(30)–TiO_2, (d) (S)-PW_{12}(15)–TiO_2, (e) (S)-PW_{12}(30)–TiO_2, and (f) (S)-PW_{12}(45)–TiO_2.

3.2.2. Effect of POMs loading

The dependence of K_{app} on POMs loading is shown in Fig. 4. 30 wt.% XW_{12} loading show the best K_{app} for X-3B degradation.

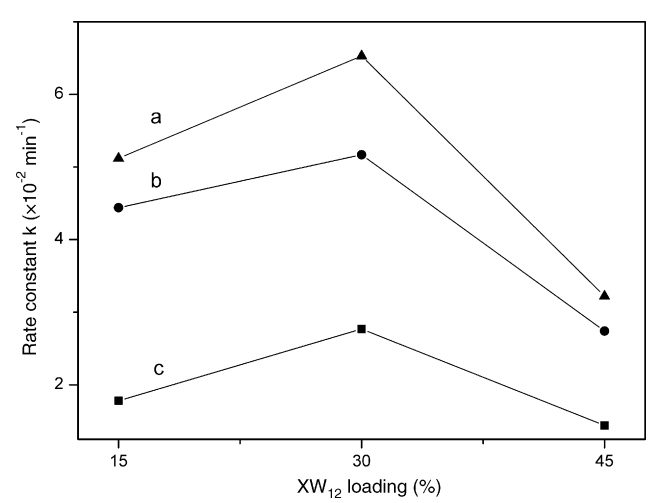

Fig. 4. Photodegradation rate constants of X-3B as function of (a) PW_{12}, (b) SiW_{12} and (c) GeW_{12} loading in (S)-XW_{12}–TiO_2 samples.

The fall of the photodegradation rate at high POMs loading was attributed to competitive adsorption between the additives and the substrates for the active site on the catalyst surface or block physically the catalyst pore by excessive amounts of additives [8]. It may also possible that inner-filter effect of POMs, which decreased the adsorption of UV, light by the photocatalysts to an extent and hindered the photodegradation [9].

3.2.3. Effect of POMs type

For XW_{12}–TiO_2 catalysts, because the molecular weights and loadings are similar even though the X is different, we can compare the activities of the three different catalysts with the same composite weight. As shown in Fig. 4, the relative activity among POMs for X-3B follows the order of PW_{12}–TiO_2 > SiW_{12}–TiO_2 > GeW_{12}–TiO_2. This indicate that central atom in the Keggin unit of POMs has a significant effect on the photocatalytic activity of the hybrid materials.

4. Conclusions

Highly dispersed XW_{12} (X = P, Si, Ge) in TiO_2 substrate were prepared by sol–gel method. Samples were characterized by FT-IR and XRD. Photocatalytic destruction of X-3B on various catalysts was investigated. The results show that: (1) the POMs could be dispersed better in TiO_2 substrate by sol–gel method than by incipient wetness method; (2) the XW_{12}–TiO_2 materials prepared by sol–gel method had a higher photoactivity performance; (3) the reaction was dependent on POMs type and loading. Among the nine (S)-XW_{12}(Y)–TiO_2 samples, (S)-PW_{12}(30)–TiO_2 showed the highest photocatalytic activity.

Acknowledgements

The financial support from the National Natural Science Foundation of China under Grant No. 20271045 and the Foundation of State Key Laboratory of Inorganic Synthesis and Preparative Chemistry of Jilin University for this work is greatly appreciated.

References

[1] M.A. Fox, M.T. Dulay, Heterogeneous photocatalysis, Chem. Rev. 93 (1993) 341–357.
[2] O. Legrim, E. Oliveros, A.M. Brown, Photochemical processes for water treatment, Chem. Rev. 93 (1993) 671–698.
[3] A. Besner, R. Gilbert, P. Tetreault, L. Lepine, J.F. Archambault, Determination of pentachlorophenol and its hydrocarbonsolvent in wood, soil, and water by gas chromatography and FT-IR spectroscopy in a single-sample treatment, Anal. Chem. 67 (1995) 442–446.
[4] J.M. Hermann, P.J. Pichat, Photo-adsorption and photo-desorptionof oxygen on highly hydroxylated TiO_2 surfaces. Part 3. Role of H_2O_2 on photodesorption of O_2^-, J. Chem. Soc., Faraday Trans. 76 (1980) 1138–1146.
[5] K. Okamoto, Y. Yamamoto, H. Tanaka, A. Haya, Kinetics of heterogeneous photocatalytic decomposition of phenol over anatase TiO_2 powder, Bull. Chem. Soc. Jpn. 58 (1985) 2023–2027.
[6] T. Yamase, Photo- and electrochromism of polyoxometalates and related materials, Chem. Rev. 98 (1998) 307–326.
[7] S.L. Zhao, Q.Y. Wu, Preparation and conductivity of hybrid materials containing undecatungstocobaltoindic heteropoly acid and polymer matrix, Mater. Lett. 60 (2006) 2650–2652.
[8] M. Yoon, J.A. Chang, Y. Kim, J.R. Choi, K. Kim, S.L. Lee, Heteropoly acid-incorporated TiO_2 colloids as novel photocatalytic systems resembling the photosynthetic reaction center, J. Phys. Chem. B 105 (2001) 2539–2545.
[9] R.R. Ozer, J.L. Ferry, Investigation of the photocatalytic activity of TiO_2–polyoxometalate systems, Environ. Sci. Technol. 35 (2001) 3242–3246.
[10] C. Chen, P. Lei, H. Ji, W. Ma, J. Zhao, Photocatalysis by titanium dioxide and polyoxometalate/TiO_2 cocatalysts. Intermediates and Mechanistic Study, Environ. Sci. Technol. 38 (2004) 329–337.
[11] Y. Yang, Y.H. Guo, C.W. Hu, C.J. Jiang, E.B. Wang, Synergistic effect of Keggin-type $[X^{n+}W_{11}O_{39}]^{(12-n)-}$ and TiO_2 in macroporous hybrid materials $[X^{n+}W_{11}O_{39}]^{(12-n)-}$–$TiO_2$ for the photocatalytic degradation of textile dyes, J. Mater. Chem. 13 (2003) 1686–1694.
[12] Q.Y. Wu, H.B. Wang, C.S. Yin, G.Y. Meng, Preparation and performance of PVA films composited with 12-tungstogermanic heteropoly acid, Mater. Lett. 50 (2001) 61–65.
[13] L. Li, Q.Y. Wu, Y.H. Guo, C.W. Hu, Nanosize and bimodal porous polyoxotungstate-anatase TiO_2 composites: Preparation and photocatalytic degradation of organophosphorus pesticide using visible-light excitation, Micropor. Mesopor. Mater. 87 (2005) 1–9.
[14] Q.Y. Wu, S.K. Wang, D.N. Li, X.F. Xie, Preparation and characterization of decatungstomolybdoniobogermanic heteropoly acid $H_5[GeW_{10}MoNbO_{40}]^{\bullet}20H_2O$, Inorg. Chem. Commun. 5 (2002) 308–311.
[15] J.C. Edward, C.Y. Thiel, B. Benac, J.F. Knifton, Solid-state NMR and FT-IR investigation of 12-tungstophosphoric acid supported on TiO_2, Catal. Lett. 51 (1998) 77–81.
[16] R. Sinnema, J.J. Jansen, K. Pamin, H. van Beckkum, New acid catalyst comprising heteropoly acid on a mesoporous molecular sieve MCM-41, Catal. Lett. 30 (1995) 241–252.
[17] W.G. Kim, M.W. Kim, J.H. Kim, G. Seo, Dispersion measurement of heteropoly acid supported on KIT-1 mesoporous material, Micropor. Mesopor. Mater. 57 (2003) 113–120.
[18] Q.Y. Wu, X.G. Sang, B. Liu, V.G. Ponomareva, Synthesis and performance of high-proton conductor undecatungstochromoindic heteropoly acid, Mater. Lett. 59 (2005) 123–126.
[19] M. Hu, Y. Xu, Photocatalytic degradation of textile dye X-3B by heteropolyoxometalate acids, Chemosphere 54 (2004) 431–434.